

1 **Synthesis, characterization and antiproliferative activity**  
2 **on mesothelioma cell lines of bis(carboxylato)**  
3 **platinum(IV) complexes based on picoplatin†**

4

5

6 Mauro Ravera,<sup>a</sup> Elisabetta Gabano,<sup>a</sup> Ilaria Zanellato,<sup>a</sup> Ilaria Bonarrigo,<sup>a</sup> Esther

7 Escribano,<sup>b</sup> Virtudes Moreno,<sup>b</sup> Mercè Font-Bardia,<sup>c,d</sup> Teresa Calvet<sup>c</sup> and Domenico

8 Osella <sup>\*a</sup>

9

10

11

12

13

14

15 <sup>a</sup> Dipartimento di Scienze dell'Ambiente e della Vita, Università del Piemonte Orientale

16 "Amedeo Avogadro", Viale Michel 11, 15121 Alessandria, Italy. E-mail:

17 [domenico.osella@mfn.unipmn.it](mailto:domenico.osella@mfn.unipmn.it); Fax: +39-0131-360250; Tel: +39-0131-360266

18 <sup>b</sup> Departament de Química Inorgànica, Universitat de Barcelona, Martí i Franquès 1-11,

19 08028 Barcelona, Spain

20 <sup>c</sup> Departament de Cristal·lografia, Mineralogia i Dipòsits Minerals, Universitat de

21 Barcelona, Martí i Franquès s/n, 08028 Barcelona, Spain

22 <sup>d</sup> Unitat de Difracció de RX, Centre Científic i Tecnològic de la Universitat de Barcelona

23 (CCITUB), Solé i Sabarís 1-3, 08028 Barcelona, Spain

24

25 **Abstract**

26           The synthesis and characterization of a series of picoplatin-based ( picoplatin =  
27 [PtCl<sub>2</sub>(mpy)(NH<sub>3</sub>)], mpy = 2-methylpyridine), Pt(IV) complexes with axial carboxylato  
28 ligands of increasing length are reported. The synthesis is based on the oxidation with  
29 hydrogen peroxide of picoplatin to give the *cis,cis,trans*-[PtCl<sub>2</sub>(mpy)(NH<sub>3</sub>)(OH)<sub>2</sub>]  
30 intermediate and then its transformation into the dicarboxylato complexes *cis, cis,trans*-  
31 [PtCl<sub>2</sub>(mpy)(NH<sub>3</sub>)(RCOO)<sub>2</sub>] (R = CH<sub>3</sub>(CH<sub>2</sub>)<sub>n</sub>, n = 0–4) with the corresponding anhydride.  
32 Pt(IV) complexes with n = 0–2 were selected to be tested on four malignant pleural  
33 mesothelioma (MPM) cell lines, on human mesothelial cells (HMC), and on the cisplatin-  
34 sensitive ovarian A2780 cell line along with cisplatin as a metallo-drug reference. In general,  
35 the longer the axial chain, the more cytotoxic and selective the Pt(IV) complex is. Pt(IV)  
36 analogs show good activity on the MPM cell lines, approaching or in some case bypassing  
37 that of cisplatin and represent quite promising drug candidates for the treatment of tumors  
38 whose chemoresistance is mainly based on glutathione overexpression, such as MPM.

39

40

41

42

43

44

45

46

47

48

49

50

## 51 1. INTRODUCTION

52 The basic US patent for the antitumor drug cisplatin (US 4,177,263) was issued in  
53 December 1979.<sup>1</sup> This is probably a milestone in the history of antitumoral chemotherapy  
54 considering that today cisplatin still plays a pivotal role in the systemic treatment of a variety  
55 of solid tumors.<sup>2</sup>

56 The two major problems associated with the use of cisplatin are the severe toxic side-  
57 effects (namely nephrotoxicity,<sup>3</sup> neurotoxicity<sup>4</sup> and ototoxicity<sup>5</sup>), as well as the intrinsic or  
58 acquired resistance manifested in various types of cancers.<sup>6</sup> As such, a large number of Pt(II)-  
59 based compounds structurally similar to cisplatin have been developed and tested, to increase  
60 the selectivity towards cancer cells and to limit the chemoresistance.

61 Chemoresistance is a multifactorial phenomenon, in particular the reaction of  
62 cisplatin with nucleophiles other than DNA, especially S-donor biomolecules, can cause  
63 inactivation of the drug.<sup>7</sup> For instance, cisplatin is inactivated in cells by reduced glutathione  
64 (GSH, present in millimolar concentrations in cells) and by metallothioneins (MTs, small  
65 proteins having 20 Cys groups per molecule), the main cellular detoxification agents.<sup>8</sup> It is  
66 important to recall, however, that GSH may not be the primary target of cisplatin, as reported  
67 by Gibson and coworkers.<sup>9</sup> A bulky carrier ligand coordinated to the platinum(II) core  
68 reduces the level of these undesired substitution reactions in the square-planar complexes.<sup>10</sup>  
69 This rationale prompted the design, synthesis, preclinical tests and clinical trials of cis-  
70 amminedichlorido(2-methylpyridine)platinum(II) (picoplatin, ZD0437, AMD-437), an  
71 active Pt(II) antitumor drug able to circumvent the acquired Pt-chemotherapy resistance.<sup>11</sup>  
72 The presence of the sterically demanding 2-methylpyridine (mpy) hinders the axial approach  
73 of nucleophiles to the platinum center without detriment of the level of DNA  
74 platination.<sup>12,13</sup> Picoplatin was granted orphan drug designation in 2007 for the treatment  
75 of small cell lung cancer (EU/3/07/502).

76 Platinum(IV) complexes, which undergo ligand substitution reactions much more  
77 slowly than their platinum(II) counterparts, are tested as orally administrable pro-drugs. It is

78 generally accepted that the reduction of Pt(IV) compounds can be carried out by intracellular  
79 reductants such as ascorbic acid, GSH or MTs. Pt(IV) complex is believed to be reduced to  
80 its Pt(II) active metabolite, which, in turn, will be activated by hydrolysis and bind DNA  
81 (Fig. 1).<sup>14</sup> The rational choice of axial ligands L is thus the key for modulating the  
82 lipophilicity (the ability to enter the tumor cells by passive diffusion) and the redox potential  
83 (the ability to be reduced under the hypoxic conditions typical of tumor tissues) of the Pt(IV)  
84 complexes.<sup>15</sup>

85 In this context, the choice of carboxylic anions with a carbon chain of increasing  
86 length as the axial ligands was particularly useful since a strict correlation between  
87 antiproliferative activity and length of the carbon chain was observed for other Pt(IV)  
88 complexes in vitro (at least as far as these complexes were soluble enough in water) and in  
89 vivo in mouse tumor models.<sup>16,17</sup>

90 Finally, the characteristics of the remaining A and X/L ligands determine the potency  
91 of the cytotoxic Pt(II)-metabolite that is eventually generated by reduction of the Pt(IV) parent  
92 complex (Fig. 1).<sup>18</sup>

93 It is interesting to consider the dual role of GSH, which on the one hand promotes  
94 the reduction of Pt(IV) to Pt(II), activating the pro-drug in cells, and on the other hand hinders  
95 the action of the resulting Pt(II) metabolite. Thus, the insertion of the picoplatin square-planar  
96 structure in a Pt(IV) octahedral scaffold should afford an ideal pro-drug candidate, easily  
97 reduced but hardly deactivated by GSH, often over-expressed by resistant tumor cells.

98 Malignant pleural mesothelioma (MPM) is a rare and aggressive asbestos-related  
99 cancer associated with poor prognosis. Currently, all the polychemotherapeutic protocols for  
100 MPM include Pt(II) complexes, namely cisplatin or carboplatin.<sup>19</sup> MPM cells of both  
101 phenotypes (namely epithelioid and sarcomatoid) are characterized by strong  
102 chemoresistance,<sup>20</sup> which has been ascribed mainly to mechanisms associated with GSH<sup>21</sup>  
103 and, then, represent an ideal challenge for picoplatin-based Pt(IV) compounds. It is important

104 to recall that picoplatin has been tested in a phase II trial as a second-line therapy in  
105 mesothelioma,<sup>22</sup> demonstrating a manageable tolerability profile.

106 In the present paper, the synthesis, characterization and antiproliferative activity on  
107 mesothelioma cell lines of a series of picoplatin-based Pt(IV) complexes having carboxylic  
108 acids with carbon chains of increasing length as axial ligands is reported (Fig. 2). This  
109 synthesis is based on the oxidation with hydrogen peroxide of picoplatin to give the  
110 *cis,cis,trans*-[PtCl<sub>2</sub>(mpy)(NH<sub>3</sub>)(OH)<sub>2</sub>] intermediate and then its transformation into  
111 dicarboxylato with the corresponding anhydride. Hambley and co-workers followed a  
112 similar strategy, but the specific reaction of the above said the Pt(IV) intermediate in neat  
113 acetic anhydride (at r.t. instead of 0 °C) resulted in extensive decomposition only.<sup>23</sup>

114

115

116

## 117 2. RESULTS AND DISCUSSION

### 118 Synthesis of the Pt(IV) complexes

119 Platinum(IV) complexes containing amine ligands are generally prepared by  
120 oxidation of the corresponding platinum(II) precursors using hydrogen peroxide or chlorine.  
121 Picoplatin was prepared in high yields according to a published method<sup>23</sup> involving the  
122 formation of the platinum dimeric species [Pt<sub>2</sub>I<sub>4</sub>(mpy)<sub>2</sub>] directly from [PtI<sub>4</sub>]<sup>2-</sup> and mpy in  
123 water. The reaction of the dimer with ammonia produces a mixed diiodido species, *cis*-  
124 [PtI<sub>2</sub>(mpy)(NH<sub>3</sub>)], which represents the synthon in Dhara's procedure<sup>24</sup> to obtain the  
125 desired picoplatin. Further treatment with excess hydrogen peroxide in water gave the  
126 dihydroxidoplatinum(IV) derivative.<sup>33</sup> The carboxylation reaction was carried out in neat  
127 anhydride, at low or room temperature (**1** and **2**), or in refluxing acetonitrile with the  
128 corresponding anhydride (**3–5**) affording the *bis*(carboxylato)platinum(IV) complexes in  
129 high (**1** and **2**) or moderate (**3–5**) yield (Scheme 1).

130 Single-crystal X-ray quality crystals were obtained for **2**, as described in the  
131 experimental section. The ORTEP representation with thermal ellipsoids of the structure of  
132 **2** is reported in Fig. 3, while the relevant information concerning data collection and details  
133 of structure refinement are summarized in Table 1. The molecule shows disorder in one of  
134 the two propanoato ligands: with the terminal methyl group being equally disordered over  
135 two sites (C3 and C3') and the H atoms of the adjacent carbon C2 being equally disordered  
136 over two pairs of sites.

137 The coordination geometry around platinum is octahedral, as expected for oxidation  
138 state IV. The equatorial plane is occupied by two chloride atoms [Pt–Cl1 2.311(1) and Pt–  
139 Cl2 2.319(1) Å] and two ammine groups [Pt–N1 2.050(5) and Pt–N2 2.065(5) Å] whereas  
140 the axial positions are occupied by propanoato ligands [Pt–O1 1.993(4) and Pt–O5 2.008(4)  
141 Å]. The coordinated oxygens are slightly misaligned with respect to an ideal octahedron  
142 [O1–Pt–O3 173.2(1)]. The bond lengths and angles can be regarded as normal compared  
143 with those described in the literature. The non-coordinated oxygen of two of the carboxylate  
144 ligands are hydrogen-bonded to the protons of one ammine and also there are hydrogen-  
145 bonds with other molecules. This hydrogen-bonding scheme was also found in previously

146 reported crystal structures of Pt(IV) complexes.<sup>25,26</sup> Distortion of the octahedron, which is  
147 probably due to the presence of the methyl group of the picoline, is proved by the values of  
148 the angles N–Pt–N 96.1°, Cl–Pt–Cl 89.1° and O–Pt–O 173.2°.

149

## 150 **Electrochemical behavior**

151 In cyclic voltammetry (CV), complexes 1–5 show a  $2e^-$  reduction process  
152 complicated by a chemically irreversible following reaction (*i.e.*, the detachment of the two  
153 axial ligands upon reduction of octahedral Pt(IV) to square-planar Pt(II),  $E_2C$  mechanism).  
154 The peak potentials are reported in Table 2.

155 It should be noted that all picoplatin Pt(IV)-complexes but 1 showed low solubility in  
156 pure water and addition of 10% of ethanol was useful to observe a better shaped peak. The  
157 measured  $E_p$  values are identical within the experimental error for experiments with ethanol  
158 contents lower than 20%. As the percentage of the co-solvent becomes higher than 20%, the  
159  $E_p$  values decrease almost linearly (Fig. 4).

160 As previously reported for the cisplatin-, nedaplatin-, and [PtCl<sub>2</sub>(dach)]- (dach = 1,2-  
161 diaminocyclohexane) based series of Pt(IV) complexes,<sup>26</sup> the  $E_p$  values increase (becomes  
162 less negative) as the axial chain length increases. Fig. 5 shows the trends of  $E_p$  *vs.* the total  
163 number of secondary carbons (nCs) for the picoplatin-based Pt(IV) complexes in comparison  
164 with the abovementioned series of compounds. Linear relations are observed in each case ( $r$   
165  $> 0.98$ ) and the lines are almost parallel (slope = 23–27 mV).

166 In pure organic solvent Pt(IV) complexes with different axial chains show very  
167 similar  $E_p$  values, pointing out that the chain length of the carboxylato ligand does not  
168 influence *per se* the reduction potential, indeed it does not substantially alter the electronic  
169 characteristics of the Pt center, where the reduction is centered.<sup>27</sup> However, in water  
170 different solvation effects on the species involved in the  $E_2C$  reduction mechanism do  
171 influence the final  $E_p$  value. The hydrophilicity/hydrophobicity of the Pt(IV) complexes and

172 the produced fragments, in particular of the carboxylates, account for the trends shown in  
173 Fig. 4 and 5.<sup>26</sup> Thus, along with the increase in lipophilicity, the chain length of the  
174 carboxylato ligand offers a further beneficial effect on antiproliferative activity of these  
175 complexes, lowering their reduction potential.

176

## 177 **Biological tests**

178 Complexes **1–3** were selected to be tested on the cisplatin-sensitive ovarian A2780  
179 cell line, on four mesothelioma cell lines, and on human mesothelial cells (HMC), along  
180 with cisplatin as reference standard (Table 3). The heavier congeners (**4** and **5**) were barely  
181 soluble in water and required consequently a too high amount of co-solvent to perform  
182 meaningful biological tests.

183 On A2780 **1** is less potent whereas **3** has higher activity than cisplatin. A similar  
184 behavior was seen for the cisplatin-based Pt(IV) analogs.<sup>17</sup> On MPM cells complexes **1–3**  
185 show an increased activity as the carbon chain length increases, approaching or in one case  
186 bypassing that of cisplatin itself. Moreover, derivatives **1–3** always exhibit a lower resistance  
187 factor RF ( $RF = IC_{50}(\text{MM98R})/IC_{50}(\text{MM98})$ ) than cisplatin.

188 Noteworthy, it has been demonstrated that the cisplatin-resistant cell line MM98R  
189 shows a higher increase in intracellular GSH (when treated with Pt derivatives at sub-lethal  
190 concentrations) with respect to the wild counterpart MM98. This could partially explain the  
191 acquired resistance.<sup>28</sup> For this reason, the observed low RF for compounds **1–3** may be  
192 related to a generally low inactivation of Pt(IV) complexes under study, or their metabolites,  
193 by GSH (see following section).

194 In general, as previously observed for other series of homologous Pt(IV) complexes,<sup>17</sup>  
195 the longer the axial chain is, the more cytotoxic the Pt(IV) complex is. On the basis of  
196 complexes **1–3** only, the relationship between activity and length of the axial chain is  
197 confirmed.

198 Table 3 shows also the  $IC_{50}$  measured on human mesothelial cells (HMC; i.e., cells  
199 isolated from patients with no history of malignant disease, see experimental for details) and  
200 the selectivity index (SI) is defined as the ratio between  $IC_{50}$  (HMC) and the mean of  $IC_{50}$



201 on BR95, MG06, and MM98. The ability to discriminate between normal and malignant  
202 cells is of paramount importance for developing clinically applicable chemotherapeutics.  
203 Cisplatin, as expected, exhibits low selectivity (SI = 1.5), while SI increases for **1–3** as the  
204 axial chain length.

205 A longer chain means both higher lipophilicity (and in turn likely higher uptake) and  
206 higher (less negative, i.e., easier reduction)  $E_p$  values (Fig. 5). Therefore, these data are  
207 consistent with the previous finding that the cytotoxicity of Pt(IV) complexes depends on both  
208 lipophilic and electronic features.<sup>17,26</sup>

209 It is noteworthy to recall, however, that a parabolic relationship between  $IC_{50}$  and the  
210 length of the carbon chain has been reported for [Pt(carboxylato)<sub>2</sub>Cl<sub>2</sub>(1R,2R-  
211 diaminocyclohexane)] complexes.<sup>16</sup> This behavior may be due to the very low solubility in  
212 water of complexes with too long chains; the solubility is a parameter not included in the  
213 above-mentioned relationships.<sup>17</sup>

214

### 215 **Reduction with glutathione (GSH)**

216 The occurrence of reduction of complexes **1–3** by GSH, the prevailing intracellular  
217 non-protein thiol with concentrations of up to 8 mM,<sup>12</sup> was verified. Complexes were  
218 dissolved in DMSO and these solutions were quickly diluted with ultrapure water to a final  
219 1 mM compound concentration (the final content of DMSO was 1%). GSH (5 eq) was added  
220 and the behavior of the resulting solutions was monitored over 4 h at 37 °C by means of RP-  
221 HPLC and ESI-MS.

222 Both chromatograms and mass spectra indicated the disappearance of the signals  
223 relating to the Pt(IV) compounds, which was almost complete after 4 h.

224 ESI-MS analyses of the freshly prepared solutions of each compound with GSH  
225 showed the presence of unreacted Pt(IV) and solvated picoplatin  
226 [PtCl(DMSO)(mpy)(NH<sub>3</sub>)]<sup>+</sup>. During the reduction of the Pt(IV) complexes other Pt(II)  
227 metabolites can be observed corresponding to the retention of the original axial ligands. In  
228 particular, in case of complex **3** it has been possible to identify low amounts of the

229 [Pt(butanoato)Cl(mpy)(NH<sub>3</sub>)] species and relatively higher quantities of the corresponding  
230 solvated species [Pt(butanoato)(DMSO)(mpy)(NH<sub>3</sub>)]<sup>+</sup>. Therefore, the reduction is  
231 associated with some rearrangements according to Gibson and co-workers<sup>18</sup> who  
232 demonstrated that the reduction of complexes like *cis,trans,cis*-  
233 [Pt<sup>IV</sup>Cl<sub>2</sub>(CH<sub>3</sub>CO<sub>2</sub>)<sub>2</sub>(NH<sub>3</sub>)(amine)] yielded the expected *cis*-[Pt<sup>II</sup>Cl<sub>2</sub>(NH<sub>3</sub>)(amine)]  
234 metabolite, along with other Pt(II) complexes containing one or two carboxylate ligands.  
235 Likely, the reduction proceeds by several pathways where only am(m)ines are constantly  
236 maintained in the coordination sphere. The reduction was found to follow a pseudo-first-  
237 order kinetic, as previously reported for several Pt(IV) complexes (see for instance *bis*-  
238 (acetato) (1-adamantylamine) amminedichloroplatinum(IV), coded as LA-12, structurally  
239 very similar to **1**).<sup>29</sup> The linearization of the data points over a 2 h time interval gave the  
240 following half-time of reduction: 32 min for **3**, 30 min for **2** and 25 min for **1**. It is important  
241 recall that an “easy” reduction (from a thermodynamic point of view) it is not always related  
242 with a short reduction time.<sup>14a,30,31</sup> In fact, Gibson *et al.* found that reduction of the Pt(IV)  
243 analogs of oxaliplatin with two axial carboxylate ligands is extremely slow while reduction  
244 of their dihydroxido analogs is much faster. However, the reduction potential of the former  
245 is higher than the latter.<sup>32</sup> For this behavior it was suggested that the reductive elimination  
246 reaction occurs *via* an attack by the reductant *via* halido- or oxygen-bridge electron  
247 transfer.<sup>14a,31</sup> The interaction between the reducing agent and the axial ligand, and hence  
248 the reduction time, follow the order Cl, OH > COOH.

249 In the actual case, as the *t*<sub>1/2</sub> are very similar, the reduction potential appears to be the  
250 paramount factor influencing IC<sub>50</sub>. Picoplatin-based Pt(IV) complexes can then be reduced  
251 by GSH to produce active Pt(II) metabolites, supporting the general view of “activation by  
252 reduction” mechanism. Moreover, the resulting Pt(II) metabolites always contain the mpy  
253 ligand, which guarantees a low inactivation of the complex by GSH. This is the reason of  
254 the good antiproliferative activity of **1–3** observed on the cisplatin resistant MM98R cell  
255 line.

256

### 257 3. EXPERIMENTAL

258 All chemicals (analytical grade) were obtained from Aldrich, except  $K_2PtCl_4$  from  
259 Alfa Aesar, and used as received. Picoplatin<sup>23</sup> and *cis,cis,trans*- $[PtCl_2(mpy)(NH_3)(OH)_2]$ <sup>33</sup>  
260 were prepared according to literature procedures. Elemental analyses were carried out with  
261 a EA3000 CHN Elemental Analyzer (EuroVector, Milano, Italy). Platinum was quantified  
262 by means of a Spectro Genesis ICP-OES spectrometer (Spectro Analytical Instruments,  
263 Kleve, Germany) equipped with a crossflow nebulizer. In order to quantify the platinum  
264 concentration the Pt 299.797 nm line was selected. A platinum standard stock solution of  
265 1000 mg L<sup>-1</sup> was diluted in 1.0% v/v nitric acid to prepare calibration standards. The  
266 elemental analyses and Pt content were within  $\pm 0.3\%$  absolute of the theoretical value.

267 The multinuclear NMR spectra were measured on a JEOL Eclipse Plus operating at  
268 400 MHz (<sup>1</sup>H), 100.5 MHz (<sup>13</sup>C), and 85.9 MHz (<sup>195</sup>Pt with a spectral window of 1200  
269 ppm), respectively (Fig. 6). <sup>1</sup>H and <sup>13</sup>C NMR chemical shifts were reported in parts per  
270 million referenced to solvent resonances. <sup>195</sup>Pt NMR spectra were recorded using a solution  
271 of  $K_2PtCl_4$  in saturated aqueous KCl as external reference. The shift for  $K_2[PtCl_4]$  was  
272 adjusted to  $-1628$  ppm relative to  $Na_2[PtCl_6]$  ( $\delta = 0$  ppm).

273 Electrospray ionization mass spectra (ESI-MS) were obtained using a Micromass  
274 ZMD mass spectrometer. Typically, a dilute solution of compound in acetone–methanol 1 :  
275 99 was delivered directly to the spectrometer source at 0.01 mL min<sup>-1</sup>, using a Hamilton  
276 microsyringe controlled by a single-syringe infusion pump. The nebulizer tip operated at  
277 3000–3500 V and 150 °C, with nitrogen used both as a drying and as a nebulizing gas. The  
278 cone voltage was 30 V. Quasi-molecular ion peaks  $[M+H]^+$  or sodiated  $[M+Na]^+$  peaks were  
279 assigned on the basis of the  $m/z$  values and of the simulated isotope distribution patterns.

280

281

282

283

284 **Synthesis of *trans,cis,cis*-[Pt(acetato)<sub>2</sub>Cl<sub>2</sub>(mpy)(NH<sub>3</sub>)], 1**

285 *cis,cis,trans*-[PtCl<sub>2</sub>(mpy)(NH<sub>3</sub>)(OH)<sub>2</sub>] (107 mg, 0.261 mmol) was suspended in neat  
286 acetic anhydride (243 μL, 2.57 mmol) at 0 °C. Then the mixture was stirred at room  
287 temperature in the dark for 4 d. The final pale yellow precipitate was separated by  
288 centrifugation and washed with diethyl ether and dried *in vacuo* (116 mg, 90%). <sup>1</sup>H NMR  
289 (400 MHz; D<sub>2</sub>O): δ 8.65 (H6, dd, <sup>3</sup>J = 6.22 Hz, <sup>4</sup>J = 1.28 Hz, 1H), 8.06 (H4, td, <sup>3</sup>J = 7.69  
290 Hz, <sup>4</sup>J = 1.28 Hz, 1H), 7.57 (H3, dd, <sup>3</sup>J = 7.69 Hz, <sup>4</sup>J = 1.64 Hz, 1H), 7.49 (H5, td, <sup>3</sup>J = 6.96  
291 Hz, <sup>4</sup>J = 1.64 Hz, 1H), 2.77 (H2, s, 3H), 2.14 (H8, s, 3H) ppm; <sup>13</sup>C NMR (100.5 MHz;  
292 D<sub>2</sub>O): δ 181.45 (C7, Cquat), 161.50 (C2, Cquat), 151.37 (C6, CH), 142.26 (C4, CH), 129.75  
293 and 124.91 (C3 and C5, 2 × CH), 23.26 and 22.61 (C1 and C8, 2 × CH<sub>3</sub>) ppm; <sup>195</sup>Pt NMR  
294 (85.9 MHz; D<sub>2</sub>O): δ 1365 ppm. ESI-MS (methanol : acetone 99 : 1) 493.15 (65.42%), 494.00  
295 (74.32%), 495.12 (100.00%), 495.98 (54.50%), 497.20 (58.95%), 498.23 (13.97%), 499.30  
296 (15.71%) m/z, calcd for C<sub>10</sub>H<sub>17</sub>Cl<sub>2</sub>N<sub>2</sub>O<sub>4</sub>Pt m/z: 493.02 (65.46%), 494.02 (74.20%), 495.02  
297 (100.00%), 496.02 (54.55%), 497.02 (59.01%), 498.02 (13.94%), 499.02 (15.76%) [M+H]<sup>+</sup>.

298

299 **Synthesis of *cis,cis,trans*-[PtCl<sub>2</sub>(mpy)(NH<sub>3</sub>)(propanoato)<sub>2</sub>], 2**

300 *cis,cis,trans*-[PtCl<sub>2</sub>(mpy)(NH<sub>3</sub>)(OH)<sub>2</sub>] (121 mg, 0.295 mmol) was added to neat  
301 propanoic anhydride (583 μL, 4.55 mmol) and allowed to react for 5 d at room temperature  
302 in the dark. The mixture was then centrifuged and the pale yellow precipitate was washed  
303 with diethyl ether and dried *in vacuo* (134 mg, 87%). <sup>1</sup>H NMR (400 MHz; acetone-d<sub>6</sub>) δ:  
304 8.88 (H6, dd, <sup>3</sup>J = 6.22 Hz; <sup>4</sup>J = 1.46 Hz, 1H), 8.10 (H4, td, <sup>3</sup>J = 7.69 Hz, <sup>4</sup>J = 1.46 Hz, 1H),  
305 7.62 (H3 and H5, m, 2H), 3.27 (NH<sub>3</sub>, m, 3H), 2.86 (H1, s, 3H), 2.29 (H8, quart, <sup>3</sup>J = 7.69  
306 Hz, 2H), 0.98 (H9, t, <sup>3</sup>J = 7.69 Hz, 3H) ppm; <sup>13</sup>C NMR (100.5 MHz; acetone-d<sub>6</sub>) δ: 182.82  
307 (C7, Cquat), 161.69 (C2, Cquat), 151.89 (C6, CH), 138.67 (C4, CH), 129.10 and 123.44 (C3  
308 and C5, 2 × CH), 30.01 (C8, CH<sub>2</sub>), 23.16 (C1, CH<sub>3</sub>), 9.59 (C9, CH<sub>3</sub>) ppm; <sup>195</sup>Pt NMR (85.9  
309 MHz; acetone-d<sub>6</sub>) δ: 1399 ppm; ESI-MS (methanol : acetone 99 : 1) 521.13 (64.34%),

310 522.01 (74.48%), 523.10 (100.00%), 524.15 (55.83%), 525.31 (59.21%), 526.14 (15.00%),  
311 527.07 (15.78%) m/z, calcd for C<sub>12</sub>H<sub>21</sub>Cl<sub>2</sub>N<sub>2</sub>O<sub>4</sub>Pt m/z: 521.05 (64.36%), 522.05 (74.44%),  
312 523.05 (100.00%), 524.05 (55.88%), 525.05 (59.28%), 526.05 (15.04%), 527.05 (15.81%)  
313 [M+H]<sup>+</sup>.

314

### 315 **Synthesis of *trans,cis,cis*-[Pt(butanoato)<sub>2</sub>Cl<sub>2</sub>(mpy)(NH<sub>3</sub>)], 3**

316 *cis,cis,trans*-[PtCl<sub>2</sub>(mpy)(NH<sub>3</sub>)(OH)<sub>2</sub>] (157 mg, 0.383 mmol) was dissolved in  
317 acetonitrile (20 mL). Butanoic anhydride (644 μL, 3.82 mmol) was then added. The mixture  
318 was refluxed for 24 h. The resulting yellow solution was dried under reduced pressure. The  
319 residual oil was dissolved in few mL of acetone and precipitated with diethyl ether to get a  
320 pale yellow powder (158 mg, 75%). <sup>1</sup>H NMR (400 MHz; acetone-d<sub>6</sub>) δ: 8.90 (H6, dd, <sup>3</sup>J =  
321 6.40 Hz, <sup>4</sup>J = 1.46 Hz, 1H), 8.11 (H4, td, <sup>3</sup>J = 7.69 Hz, <sup>4</sup>J = 1.46 Hz, 1H), 7.60 (H3 and H5,  
322 m, 2H), 2.86 (H1, s, 3H), 2.24 (H8, m, 2H), 1.53 (H9, m, 2H), 0.88 (H10, t, <sup>3</sup>J = 7.50 Hz,  
323 3H) ppm; <sup>13</sup>C NMR (100.5 MHz; acetone-d<sub>6</sub>) δ: 182.07 (C7, C<sub>quat</sub>), 161.73 (C2, C<sub>quat</sub>),  
324 152.12 (C6, CH), 141.46 (C4, CH), 129.00 and 123.98 (C3 and C5, 2 × CH), 38.86 (C8,  
325 CH<sub>2</sub>), 23.25 (C1, CH<sub>3</sub>), 19.13 (C9, CH<sub>2</sub>), 13.24 (C10, CH<sub>3</sub>) ppm; <sup>195</sup>Pt NMR (85.9 MHz;  
326 acetone-d<sub>6</sub>) δ: 1407 ppm; ESI-MS (methanol : acetone 99 : 1) 549.12 (63.23%), 550.15  
327 (74.58%), 551.06 (100.00%), 552.03 (57.23%), 553.14 (59.55%), 554.11 (16.16%), 555.05  
328 (15.91%) m/z, calcd for C<sub>14</sub>H<sub>25</sub>Cl<sub>2</sub>N<sub>2</sub>O<sub>4</sub>Pt m/z: 549.08 (63.26%), 550.08 (74.62%), 551.08  
329 (100.00%), 552.08 (57.21%), 553.08 (59.53%), 554.08 (16.12%), 555.08 (15.89%) [M+H]<sup>+</sup>.

330

### 331 **Synthesis of *cis,cis,trans*-[PtCl<sub>2</sub>(NH<sub>3</sub>)(mpy)(pentanoato)<sub>2</sub>], 4**

332 *cis,cis,trans*-[PtCl<sub>2</sub>(mpy)(NH<sub>3</sub>)(OH)<sub>2</sub>] (140 mg, 0.341 mmol) was dissolved in  
333 acetonitrile (20 mL). Pentanoic anhydride (700 μL, 3.44 mmol) was then added and the  
334 mixture was refluxed for 24 h. The resulting yellow solution was dried under reduced  
335 pressure. The residual oil was re-crystallized from methanol–diethyl ether and washed with

336 diethyl ether to get a pale yellow powder (98 mg, 50%). <sup>1</sup>H NMR (400 MHz; acetone-d<sub>6</sub>) δ:  
337 8.90 (H6, dd, <sup>3</sup>J = 6.59 Hz, <sup>4</sup>J = 1.10 Hz, 1H), 8.11–7.50 (H3, H4 and H5, m, 3H), 3.29  
338 (NH<sub>3</sub>, m, 3H), 2.86 (H1, s, 3H), 2.26 (H8, m, 2H), 1.49 (H9, m, 2H), 1.31 (H10, m, 2H),  
339 0.84 (H11, m, 3H) ppm; <sup>13</sup>C NMR (100.5 MHz; acetone-d<sub>6</sub>) δ: 182.21 (C7, C<sub>quat</sub>), 161.75  
340 (C2, C<sub>quat</sub>), 152.08 (C6, CH), 141.50 (C4, CH), 129.06 and 124.00 (C3 and C5, 2 × CH),  
341 36.71 (C8, CH<sub>2</sub>), 27.91 (C9, CH<sub>2</sub>), 23.26 and 22.07 (C1 and C10, CH<sub>3</sub> and CH<sub>2</sub>), 13.33  
342 (C11, CH<sub>3</sub>) ppm; <sup>195</sup>Pt NMR (85.9 MHz; acetone-d<sub>6</sub>) δ: 1408 ppm; ESI-MS (methanol :  
343 acetone 99 : 1) 577.03 (62.23%), 578.16 (74.75%), 579.14 (100.00%), 580.08 (58.52%),  
344 581.16 (59.80%), 582.05 (17.24%), 583.07 (16.02%) m/z, calcd for C<sub>16</sub>H<sub>29</sub>Cl<sub>2</sub>N<sub>2</sub>O<sub>4</sub>Pt m/z:  
345 577.11 (62.21%), 578.12 (74.78%), 579.11 (100.00%), 580.11 (58.50%), 581.11 (59.84%),  
346 582.11 (17.20%), 583.11 (16.00%) [M+H]<sup>+</sup>.

347

#### 348 **Synthesis of *cis,trans,cis*-[PtCl<sub>2</sub>(hexanoato)<sub>2</sub>(mpy)(NH<sub>3</sub>)], 5**

349 *cis,cis,trans*-[PtCl<sub>2</sub>(mpy)(NH<sub>3</sub>)(OH)<sub>2</sub>] (148 mg, 0.361 mmol) was dissolved in  
350 acetonitrile (20 mL). Hexanoic anhydride (428 μL, 1.80 mmol) was then added and the  
351 mixture was refluxed for 24 h. The resulting yellow solution was dried under reduced  
352 pressure. The residual oil was re-crystallized from methanol–diethyl ether and washed with  
353 diethyl ether to get a pale yellow powder (77 mg, 35%). <sup>1</sup>H NMR (400 MHz; acetone-d<sub>6</sub>) δ:  
354 8.90 (H6, dd, <sup>3</sup>J = 6.59 Hz, <sup>4</sup>J = 1.10 Hz, 1H), 8.10–7.40 (H3, H4 and H5, m, 3H), 3.29  
355 (NH<sub>3</sub>, m, 3H), 2.86 (H1, s, 3H), 2.26 (H8, m, 2H), 1.51 (H9, m, 2H), 1.29 (H10 and H11, m,  
356 4H), 0.86 (H12, t, 3H) ppm; <sup>13</sup>C NMR (100.5 MHz; acetone-d<sub>6</sub>) δ: 182.23 (C7, C<sub>quat</sub>), 161.76  
357 (C2, C<sub>quat</sub>), 152.10 (C6, CH), 141.52 (C4, CH), 129.10 and 124.08 (C3 and C5, 2 × CH),  
358 36.93 (C8, CH<sub>2</sub>), 30.91 (C10, CH<sub>2</sub>), 24.42 (C9, CH<sub>2</sub>), 23.26 and 22.4 (C1 and C11, CH<sub>3</sub> and  
359 CH<sub>2</sub>), 13.47 (C12, CH<sub>3</sub>) ppm; <sup>195</sup>Pt NMR (85.9 MHz; acetone-d<sub>6</sub>) δ: 1408 ppm; ESI-MS  
360 (methanol : acetone 99 : 1) 605.16 (61.14%), 606.11 (74.95%), 607.13 (100.00%), 608.18  
361 (59.80%), 609.18 (60.10%), 610.09 (18.24%), 611.10 (16.14%) m/z, calcd for  
362 C<sub>18</sub>H<sub>33</sub>Cl<sub>2</sub>N<sub>2</sub>O<sub>4</sub>Pt m/z: 605.14 (61.17%), 606.15 (74.92%), 607.15 (100.00%), 608.15  
363 (59.78%), 609.15 (60.14%), 610.15 (18.26%), 611.15 (16.12%) [M+H]<sup>+</sup>.

## 364 X-Ray structure

365 Yellow crystals of **2** were obtained from slow diffusion of ether into an acetone  
366 solution at room temperature. Suitably sized crystals were selected for X-ray single-crystal  
367 diffraction measurements. A prismatic crystal ( $0.1 \times 0.1 \times 0.2$  mm) was selected and  
368 mounted on a MAR345 (Marresearch GmbH, Norderstedt, Germany) diffractometer with an  
369 image plate detector. A summary of the crystal data, structure solution and refinement  
370 parameters are given in Table 1. Bond lengths ( $\text{\AA}$ ) and angles ( $^\circ$ ) are reported in the ESI,<sup>†</sup>  
371 along with atomic coordinates ( $\times 10^4$ ) and equivalent isotropic displacement parameters ( $\text{\AA}^2$   
372  $\times 10^3$ ), anisotropic displacement parameters ( $\text{\AA}^2 \times 10^3$ ), hydrogen coordinates ( $\times 10^4$ ) and  
373 isotropic displacement parameters ( $\text{\AA}^2 \times 10^3$ ), and hydrogen bonds ( $\text{\AA}$  and  $^\circ$ ).<sup>†</sup>

374 Unit-cell parameters were determined from 7652 reflections ( $3 < \theta < 31^\circ$ ) and refined  
375 by least-squares method. Intensities were collected with graphite monochromatized  
376 molybdenum  $K\alpha$  radiation. 15 764 reflections were measured in the range  $32.38 \leq \theta \leq$   
377  $5022$ , 4676 of which were non-equivalent by symmetry ( $R_{\text{int}}(\text{on } I) = 0.049$ ). 4676  
378 reflections were assumed as observed applying the condition  $I > 2\sigma(I)$ . Lorentz-polarization  
379 and absorption corrections were made. The structure was solved by direct methods, using  
380 the SHELXS computer program and refined by full-matrix least-squares method with the  
381 SHELX97 computer program,<sup>34</sup> using 15 764 reflections (very negative intensities were not  
382 assumed). The function minimized was  $\Sigma w||F_o|^2 - |F_c|^2|^2$ , where  $w = [\sigma^2(I) + (0.0470P)^2 +$   
383  $1.2647P]^{-1}$ , and  $P = (|F_o|^2 + 2|F_c|^2)/3$ . Values of  $f$ ,  $f'$  and  $f''$  were taken from International  
384 Tables of X-ray crystallography.<sup>35</sup> All H atoms were computed and refined, using a riding  
385 model, with an isotropic temperature factor equal to 1.2 times the equivalent temperature  
386 factor of the atom which are linked. The final R(on F) factor was 0.031,  $wR(\text{on } |F|^2) = 0.083$   
387 and goodness-of-fit = 1.100 for all observed reflections. Number of refined parameters was  
388 199. Maximum and mean shift/esd = 0.00. Maximum and minimum peaks in final difference  
389 synthesis were 1.302 and  $-2.089 \text{ e}\text{\AA}^{-3}$ , respectively.

390

391

## 392 **Electrochemical measurements**

393 An Autolab PGSTAT12 electrochemical analyzer (Eco Chemie, Utrecht, The  
394 Netherlands) interfaced to a personal computer running GPES 4.9 electrochemical software  
395 was used for the electrochemical measurements. A standard three-electrode cell was  
396 designed to allow the tip of the reference electrode (Ag/AgCl, 3M KCl) to closely approach  
397 the working electrode (a glassy carbon, GC, disk, diameter 0.1 cm, sealed in epoxy resin).  
398 The GC working electrode was polished with alumina followed by diamond paste, then  
399 rinsed with distilled water and dried. This process yielded an almost completely reproducible  
400 surface for all experiments. All measurements were carried out under nitrogen in 0.05 M  
401 phosphate buffer (PB, pH 7.4) containing NaCl 0.15 M and different percentages of ethanol  
402 as co-solvent. Metal complex solutions were  $5.0 \times 10^{-4}$  M. The temperature of the solution  
403 was kept constant ( $25 \pm 1$  °C) by circulation of a thermostated water–ethanol mixture  
404 through a jacketed cell. Positive-feedback iR compensation was applied routinely. All  
405 potentials are measured at  $0.2 \text{ V s}^{-1}$  scan rate and reported vs. normal hydrogen electrode  
406 (NHE).

407

## 408 **Reduction with glutathione**

409 RP-HPLC for the reduction study were performed using a Waters HPLC-MS  
410 instrument equipped with Alliance 2695 separations module, 2487 Dual lambda absorbance  
411 detector, 3100 mass Detector. The chromatographic conditions were:<sup>36</sup> silica-based C18 gel  
412 as the stationary phase (5- $\mu\text{m}$  Gemini<sup>®</sup> C<sup>18</sup> column  $25 \times 3$  mm ID); mobile phase containing  
413 15 Mm HCOOH : MeOH 50 : 50 for **3**, 60 : 40 for **2** and 70 : 30 for **1** (flow rate =  $0.5 \text{ mL}$   
414  $\text{min}^{-1}$ ; isocratic elution, UV-vis detector set at 210 nm). ESI-MS measurements ( positive  
415 ion mode) were performed with instrumental settings reported above.

416

## 417 **Biological tests**

418 All compounds were tested on three primary cell lines, derived from pleural effusion  
419 of previously untreated patients suffering from MPM, called BR95 and MG06 (epithelioid)  
420 and MM98 (sarcomatoid), and on a cisplatin-resistant cell line derived from wild type MM98



421 by exposure to sub-lethal concentrations of cisplatin for several months, called MM98R.<sup>37</sup>  
422 HMC were obtained from the biobank of the Hospital of Alessandria (Pathology Unit).  
423 HMCs were isolated from patients with no history of malignant disease.<sup>38</sup> HMCs and  
424 epithelioid MPM cells were grown in F10 Ham medium, while Dulbecco Modified Eagle's  
425 Medium (DMEM) was used for sarcomatoid MPM cells. Human ovarian carcinoma cells  
426 A2780 were purchased from ECACC (European Collection of Cell Cultures, UK) and grown  
427 in RPMI-1640 medium. Media were obtained from Gibco (Invitrogen Life Science, San  
428 Giuliano Milanese, Italy) supplemented with L-glutamine 2 mM, penicillin 100 IU mL<sup>-1</sup>,  
429 streptomycin (100 mg L<sup>-1</sup>) and 10% fetal bovine serum (FBS) at 37 °C in a 5% CO<sub>2</sub>  
430 humidified chamber. A quantity of 2–5 × 10<sup>3</sup> cells per well were seeded onto 96-well flat-  
431 bottom plates and allowed to attach 24 h before drug treatment. Compounds were dissolved  
432 in DMSO to final concentration 5 mM for **1**; and 2.5 mM for **2** and **3**. The mother solutions  
433 were serially diluted in complete medium, never exceeding 0.5% total DMSO, this  
434 concentration was found to be non-toxic to the cell tested. Cisplatin (Sigma) was dissolved  
435 in 0.9% NaCl and sterile filtered. Aqueous HCl was added to the cisplatin stock solution (1  
436 mM) up to pH 3, in order to avoid hydrolysis during storage at –80 °C. Challenge with the  
437 compounds was performed for 72 h continuous treatment.

438 At the end of the experiment, the [3-(4,5-dimethylthiazol-2-yl)-5-(3-  
439 carboxymethoxyphenyl)-2-(4-sulfophenyl)-2H-tetrazolium] inner salt (MTS) assay was  
440 performed using a commercial kit (CellTiter Aqueous Solution, Promega, Milan, Italy),  
441 according to the manufacturer's instructions; absorbance values were recorded at 490/620  
442 nm by a spectrophotometric plate reader (Sirio S, SEAC, Florence, Italy) and corrected by  
443 subtraction of the absorbance of MTS alone.

444 Residual cell viability was also evaluated by means of the resazurin reduction  
445 assay.<sup>39</sup> Briefly, cells were seeded in black sterile tissue-culture treated 96-well plates. At  
446 the end of the treatment, the viability was assayed with 10 µg mL<sup>-1</sup> resazurin (Acros  
447 Chemicals, France) in fresh medium for 1 h at 37 °C, and the amount of the reduced product,  
448 resorufin, was measured by means of fluorescence using an excitation wavelength of 550  
449 nm and an emission wavelength of 585 nm with a Tecan Infinite F200 plate reader (Tecan  
450 Austria).

451           In each experiment, the cells were challenged with the drug candidates at different  
452 concentrations and the final data were calculated from at least three replicates of the same  
453 experiment carried out in triplicate. The absorbance or fluorescence of 8 wells containing  
454 medium without cells were used as blank. The absorbance or fluorescence data were  
455 normalized to 100% cell viability for non-treated cells, half inhibiting concentration (IC<sub>50</sub>),  
456 defined as the concentration of the drug reducing cell viability by 50%, was obtained from  
457 the dose–response sigmoid using Origin Pro (version 8, Microcal Software, Inc.,  
458 Northampton, MA, USA).

459

460

461

#### 462 4. CONCLUSIONS

463 The synthesis and characterization of a series of picoplatin-based Pt(IV) complexes  
464 with axial carboxylato ligands of increasing length are reported. The oxidation of picoplatin  
465 with hydrogen peroxide to give the *cis,cis,trans*-[PtCl<sub>2</sub>(mpy)(NH<sub>3</sub>)(OH)<sub>2</sub>] intermediate is  
466 followed by the transformation into dicarboxylato complexes *cis,cis,trans*-  
467 [PtCl<sub>2</sub>(mpy)(NH<sub>3</sub>)(RCOO)<sub>2</sub>] **1–5** by reaction with the corresponding anhydride. Complexes  
468 **1–3** were selected to be tested, along with cisplatin as the prototypal metallo-drug, on four  
469 MPM cell lines, on HMC, and on the cisplatin-sensitive ovarian A2780 cell line. The longer  
470 the axial chain, the more cytotoxic and selective the corresponding Pt(IV) complex is,  
471 approaching or overcoming the performance of cisplatin.

472 When complexes **1–3** reacted with GSH, the formation of the corresponding Pt(II)  
473 species (with quite similar *t*<sub>1/2</sub> ranging between 25 and 32 min) is observed, supporting the  
474 general view of “activation by reduction” mechanism. As the cisplatin-resistant cell line  
475 MM98R exhibits high levels of intracellular GSH, especially during platinum-drug  
476 treatment, the observed low RF for compounds **1–3** may be related to a generally low  
477 inactivation of reduced Pt(II) metabolites.

478 In conclusion, provided that tests on monolayer cell culture are only indicative,  
479 especially for Pt(IV) pro-drug candidates, and required to be corroborated by experiments on  
480 spheroids and *in vivo*, the insertion of the picoplatin moiety in the octahedral structure of  
481 Pt(IV) with additional axial carboxylato ligands affords complexes quite promising for  
482 treatment of tumors whose chemoresistance is mainly based on GSH overexpression, such  
483 as mesothelioma.

484

485

486 **5. ACKNOWLEDGEMENTS**

487           We are indebted to the CRT Foundation (Turin) and Provincia di Alessandria for  
488 financial support, and to Professor P.-G. Betta (Mesothelioma Biobank Reference Center,  
489 Alessandria National Hospital) for providing cell lines. We acknowledge the EU-COST  
490 Action D39 (Metallo-Drug Design and Action), and the Inter-University Consortium for  
491 Research on the Chemistry of Metal Ions in Biological Systems (CIRCMSB, Bari, Italy)  
492 within this research was carried out. EE thanks the Spanish Ministry of Science and  
493 Innovation for a PhD grant associated to the Project CTQ2008-02064. Finally, we thank the  
494 three Referees for their stimulating criticisms and suggestions.

495

496

497

498

499

500

## 501 6. NOTES AND REFERENCES

- 502 1 R. I. Eisenstein and D. S. Resnick, *Nat. Biotechnol.*, 2001, 19, 881–882.
- 503 2 (a) Non-Small Cell Lung Cancer Collaborative Group, *Br. Med. J.*, 1995, 311, 899–  
504 909; (b) R. S. Go and A. A. Adjei, *J. Clin. Oncol.*, 1999, 17, 409–422; (c) M. Q.  
505 Bagstrom, T. E. Stinchcombe, D. B. Fried, C. Poole, T. A. Hensing and M. A.  
506 Socinski, *J. Thorac. Oncol.*, 2007, 2, 845–853; (d) K. Hotta, K. Matsuo, H. Ueoka, K.  
507 Kiura, M. Tabata and M. Tanimoto, *J. Clin. Oncol.*, 2004, 22, 3852–3859.
- 508 3 N. Pabla and Z. Dong, *Kidney Int.*, 2008, 73, 994–1007.
- 509 4 S. R. McWhinney, R. M. Goldberg and H. L. McLeod, *Mol. Cancer Ther.*, 2009, 8,  
510 10–16.
- 511 5 J. H. van den Berg, J. H. Beijnen, A. J. M. Balm and J. H. M. Schellens, *Cancer Treat.*  
512 *Rev.*, 2006, 32, 390–397.
- 513 6 B. Koberle, M. T. Tomicic, S. Usanova and B. Kaina, *Biochim Biophys. Acta, Rev.*  
514 *Cancer*, 2010, 1806, 172–182.
- 515 7 J. Reedijk, *Chem. Rev.*, 1999, 99, 2499–2510.
- 516 8 (a) M. A. Fuertes, C. Alonso and J. M. Pérez, *Chem. Rev.*, 2003, 103, 645–662; (b) J.  
517 Reedijk and J. M. Teuben, in *Cisplatin. Chemistry and Biochemistry of a Leading*  
518 *Anticancer Drug*, ed. B. Lippert, Wiley-VCH, Weinheim, 1999, pp. 339–362; (c) M.  
519 G. Cherian, S. B. Howell, N. Imura, C. D. Klaassen, J. Koropatnick, J. S. Lazo and M.  
520 P. Waalkes, *Toxicol. Appl. Pharmacol.*, 1994, 126, 1–5.
- 521 9 Y. Kasherman, S. Sturup and D. Gibson, *J. Med. Chem.*, 2009, 52, 4319–4328.
- 522 10 F. Basolo, F. J. Chatt, H. B. Gray, R. G. Pearson and B. L. J. Shaw, *J. Chem. Soc.*,  
523 1961, 2207–2215.
- 524 11 L. Kelland, *Nat. Rev. Cancer*, 2007, 7, 573–584.
- 525 12 Y. Chen, Z. Guo, S. Parsons and P. J. Sadler, *Chem.–Eur. J.*, 1998, 4, 672–676.
- 526 13 (a) J. F. Holford, F. I. Raynaud, B. A. Murrer, K. Grimaldi, J. A. Hartley, M. J. Abrams  
527 and L. R. Kelland, *Anti-Cancer Drug Des.*, 1998, 13, 1–18; (b) F. I. Raynaud, F. E.  
528 Boxall, P. M. Goddard, P. Valenti, M. Jones, M. A. Murrer, M. J. Abrams and L. R.

- 529 Kelland, *Clin. Cancer Res.*, 1997, 3, 2063–2074.
- 530 14 (a) M. D. Hall and T. W. Hambley, *Coord. Chem. Rev.*, 2002, 32, 49–67; (b) S. Choi,  
531 S. Delaney, L. Orbai, E. J. Padgett and A. S. Hakemian, *Inorg. Chem.*, 2001, 40, 5481–  
532 5482; (c) S. Choi, R. B. Cooley, A. S. Hakemian, C. Y. Larrabee, R. C. Bunt, S. D.  
533 Maupas, J. G. Muller and C. J. Burrows, *J. Am. Chem. Soc.*, 2004, 126, 591–598; (d)  
534 S. Choi, R. B. Cooley, A. Voutchkova, C. H. Leung, L. Vastag and D. E. Knowles, *J.*  
535 *Am. Chem. Soc.*, 2005, 127, 1773–1781.
- 536 15 (a) M. D. Hall, R. A. Alderden, M. Zhang, P. J. Beale, Z. Cai, B. Lai, A. P. J. Stamp  
537 and T. W. Hambley, *J. Struct. Biol.*, 2006, 155, 38–44; (b) M. D. Hall, H. R. Mellor,  
538 R. Callaghan and T. W. Hambley, *J. Med. Chem.*, 2007, 50, 3403–3411; (c) A. M.  
539 Montaña and C. Batalla, *Curr. Med. Chem.*, 2009, 16, 2235–2260.
- 540 16 (a) L. R. Kelland, B. A. Murrer, G. Abel, C. M. Giandomenico, P. Mistry and K. R.  
541 Harrap, *Cancer Res.*, 1992, 52, 822–828; (b) S. R. Ali Khan, S. Huang, S. Shamsuddin,  
542 S. Inutsuka, K. H. Whitmire, Z. H. Siddik and A. R. Khokhar, *Bioorg. Med. Chem.*,  
543 2000, 8, 515–521.
- 544 17 P. Gramatica, E. Papa, M. Luini, E. Monti, M. B. Gariboldi, M. Ravera, E. Gabano, L.  
545 Gaviglio and D. Osella, *J. Biol. Inorg. Chem.*, 2010, 15, 1157–1169.
- 546 18 A. Nemirovski, I. Vinograd, K. Takrouri, A. Mijovilovich, A. Rompel and D. Gibson,  
547 *Chem. Commun.*, 2010, 46, 1842–1844.
- 548 19 M. Ray and H. L. Kindler, *Chest*, 2009, 136, 888–896.
- 549 20 A. A. Mujoomdar, T. R. Tilleman, W. G. Richards, R. Bueno and D. J. Sugarbaker, *J.*  
550 *Thorac. Cardiovasc. Surg.*, 2010, 140, 352–355.
- 551 21 K. Järvinen, Y. Soini, K. Kahlos and V. L. Kinnula, *Hum. Pathol.*, 2002, 33, 748–755.
- 552 22 G. Giaccone, M. E. O'Brien, M. J. Byrne, M. Bard, E. Kaukel and B. Smit, *Eur. J.*  
553 *Cancer*, 2002, 38, S19–S24.
- 554 23 A. R. Battle, R. Choi, D. E. Hibbs and T. W. Hambley, *Inorg. Chem.*, 2006, 45, 6317–  
555 6322.
- 556 24 S. C. Dhara, *Indian J. Chem.*, 1970, 8, 193–194.
- 557 25 (a) M. R. Reithofer, S. M. Valiahdi, M. A. Jakupec, V. B. Arion, A. Egger, M. Galanski

- 558 and B. K. Keppler, *J. Med. Chem.*, 2007, 50, 6692–6699; (b) W. H. Ang, S. Pilet, R.  
559 Scopelliti, F. Bussy, L. Juillerat-Jeanneret and P. J. Dyson, *J. Med. Chem.*, 2005, 48,  
560 8060–8069.
- 561 26 J. A. Platts, G. Ermondi, G. Caron, M. Ravera, E. Gabano, L. Gaviglio, G. Pelosi and  
562 D. Osella, *J. Biol. Inorg. Chem.*, 2011, 16, 361–372.
- 563 27 M. R. Reithofer, A. K. Bytzeck, S. M. Valiahd, C. R. Kowol, M. Groessl, C. G.  
564 Hartinger, M. A. Jakupec, M. Galanski and B. K. Keppler, *J. Inorg. Biochem.*, 2011,  
565 105, 46–51.
- 566 28 I. Zanellato, I. Bonarrigo, M. Sardi, M. Alessio, E. Gabano, M. Ravera and D. Osella,  
567 *ChemMedChem*, 2011, 6, 2287–2293.
- 568 29 F. Žák, J. Turánek, A. Kroutil, P. Sova, A. Mistr, A. Poullová, P. Mikolin, Z. Žák, A.  
569 Kašná, D. Záluská, J. Neča, L. Šindlerová and A. Kozubík, *J. Med. Chem.*, 2004, 47,  
570 761–763.
- 571 30 S. Choi, C. Filotto, M. Bisanzo, S. Delaney, D. Lagasee, J. L. Whitworth, A. Jusko, C.  
572 R. Li, N. A. Wood, J. Willingham, A. Schwenker and K. Spaulding, *Inorg. Chem.*,  
573 1998, 37, 2500–2504.
- 574 31 L. Chen, P. F. Lee, J. D. Ranford, J. J. Vittal and S. Y. Wong, *J. Chem. Soc., Dalton*  
575 *Trans.*, 1999, 1209–1212.
- 576 32 J. Zhang, E. Wexselblatt, T. Hambley and D. Gibson, *Chem. Commun.*, 2012, 48, 847–  
577 849.
- 578 33 C. M. Giandomenico and E. S. Y. Wong, US Pat, 6,413,953 B1, 2002
- 579 34 G. M. Sheldrick, *Acta Crystallogr., Sect. A: Found. Crystallogr.*, 2008, 64, 112–122.
- 580 35 International Tables of X-Ray Crystallography, ed. J. A. Ibers and W. C. Hamilton,  
581 Kynoch Press, Birmingham, 1976, vol. IV, pp. 99–100 and 149.
- 582 36 J. A. Platts, S. P. Oldfield, M. M. Reif, A. Palmucci, E. Gabano and D. Osella, *J. Inorg.*  
583 *Biochem.*, 2006, 100, 1199–1207.
- 584 37 I. Zanellato, C. D. Boidi, G. Lingua, P. Betta, S. Orecchia, E. Monti and D. Osella,  
585 *Cancer Chemother. Pharmacol.*, 2011, 67, 265–273.
- 586 38 (a) S. Orecchia, F. Schillaci, M. Salvio, R. Libener and P.-G. Betta, *Lung Cancer*,

587 2004, 45, S37–S43; (b) E. Aldieri, C. Riganti, F. Silvagno, S. Orecchia, P. G. Betta, S.  
588 Doublier, E. Gazzano, M. Polimeni, A. Bosia and D. Ghigo, *Am. J. Respir. Cell Mol.*  
589 *Biol.*, 2011, 45, 625–631.

590 39 E. Magnani and E. Bettini, *Brain Res. Protoc.*, 2000, 5, 266–272.

591

592

593

594

595

596

597

598

599



600 **Table 1** Crystal data and structure refinement for complex **2**

601

	<b>2</b>
Formula	C <sub>12</sub> H <sub>20</sub> Cl <sub>2</sub> N <sub>2</sub> O <sub>4</sub> Pt
<i>M<sub>r</sub></i>	522.29
<i>T</i> /K	123(2)
Crystal system	Monoclinic
Space group	<i>P2<sub>1</sub>/c</i>
<i>a</i> /Å	11.576(5)
<i>b</i> /Å	7.980(3)
<i>c</i> /Å	21.461(5)
$\alpha$ (°)	90
$\beta$ (°)	119.29(2)
$\gamma$ (°)	90
<i>V</i> /Å <sup>3</sup>	1729.0(11)
<i>Z</i>	4
<i>D</i> <sub>calc</sub> /g cm <sup>-3</sup>	2.006
Wavelength/Å	0.71073
Absorption coefficient/mm <sup>-1</sup>	8.438
<i>F</i> (000)	1000
Crystal size/mm	0.2 × 0.1 × 0.1
$\theta$ range for data collection (°)	2.02–32.38
Limiting indices	–16 ≤ <i>h</i> ≤ 16, –11 ≤ <i>k</i> ≤ 10, –25 ≤ <i>l</i> ≤ 25
Reflections collected/unique	15 764/5022 [ <i>R</i> <sub>int</sub> = 0.0494]
Completeness to $\theta = 25.00$	98.0%
Absorption correction	Empirical
Maximum and minimum transmission	0.43 and 0.39
Refinement method	Full-matrix least-squares on <i>F</i> <sup>2</sup>
Data/restraints/parameters	5022/4/201
Goodness-of-fit on <i>F</i> <sup>2</sup>	1.097
Final <i>R</i> indices [ <i>I</i> > 2σ( <i>I</i> )]	<i>R</i> <sub>1</sub> = 0.0308, w <i>R</i> <sub>2</sub> = 0.0826
<i>R</i> indices (all data)	<i>R</i> <sub>1</sub> = 0.0325, w <i>R</i> <sub>2</sub> = 0.0853
Largest difference peak and hole/e Å <sup>-3</sup>	1.357 and –2.169

602

603

604

605 **Table 2.** Reduction peak potentials  $E_p$  for the 1–5 series of compounds ( $[Pt] = 0.5$  mM, in  
606 0.05 M PB/0.15 M NaCl + 10% ethanol, glassy carbon working electrode)

607

Compound	$E_p$ (V vs. NHE at $0.2 \text{ V s}^{-1}$ )
1	-0.090
2	+0.048
3	+0.114
4	+0.150
5	+0.160

608

609

610

611

612 **Table 3** IC<sub>50</sub> values for 72 h of continuous treatment

613

Complex	IC <sub>50</sub> values (μM)							SI <sup>c</sup>
	A2780	BR95	MG06	MM98	MM98R	HMC	RF <sup>b</sup>	
Cisplatin	1.2 ± 0.4	6.2 ± 0.9 <sup>a</sup>	4.1 ± 1.5 <sup>a</sup>	3.2 ± 1.0 <sup>a</sup>	19.4 ± 2.8 <sup>a</sup>	6.7 ± 1.2	6.1	1.5
1	7.4 ± 1.9	17.5 ± 4.9	13.2 ± 4	12.7 ± 3	12.1 ± 1.9	22.8 ± 2.0	1.0	1.6
2	2.4 ± 1.3	15.2 ± 2.1	11.1 ± 0.6	10.1 ± 2.6	13.2 ± 2.3	21.3 ± 1.9	1.3	1.8
3	0.40 ± 0.04	5.6 ± 0.2	7.2 ± 0.8	5.6 ± 0.5	9.4 ± 0.9	18.9 ± 3.1	1.7	3.1

<sup>a</sup> Data from ref. 28. <sup>b</sup> Resistance factor RF = IC<sub>50</sub> (MM98R)/IC<sub>50</sub> (MM98). <sup>c</sup> Selectivity index SI = IC<sub>50</sub> (HMC)/mean IC<sub>50</sub> (BR95, MG06, MM98).

614

615

616

617

618 **Figures Captions**

619 **Figure 1.** A general scheme of the  $2e^-$  reduction of a generic Pt(IV) complex (A =  
620 am(m)ines, X and L = chlorides or carboxylates) according to ref. 18.

621 **Figure 2.** Sketch of picoplatin and its Pt(IV)-based derivatives.

622 **Scheme 1.** (i) **1**: neat acetic anhydride at 0 °C, then r.t. in the dark for 4 days; **2**: neat  
623 propanoic anhydride for 5 days at r.t. in the dark; butanoic (**3**), pentanoic (**4**), and hexanoic  
624 (**5**) anhydride in acetonitrile, then mixture refluxed for 24 h.

625 **Figure 3.** ORTEP representation of **2**, ellipsoids at 50% probability

626 **Figure 4.** Plot of the  $E_p$  values of **1** (empty squares) and **3** (black squares) vs. % of co-  
627 solvent ethanol.

628 **Figure 5.**  $E_p$  vs. the total number of axial secondary carbons (nCs) for the picoplatin-based  
629 Pt(IV) complexes (stars) in comparison with cisplatin-(squares), nedaplatin- (triangles), and  
630 [PtCl<sub>2</sub>(dach)]- (circles) based series of Pt(IV) complexes (see ref. 26).

631 **Figure 6.** Numbering scheme used to assign the NMR signals in complexes **1–5**.

632

633

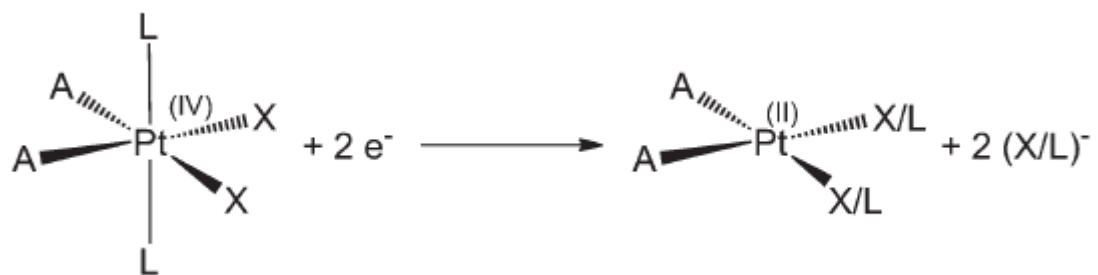
634

635

636

637 **Figure 1**

638



639

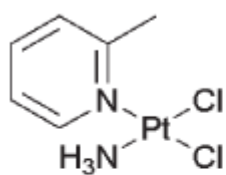
640

641

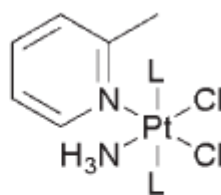
642

643 **Figure 2**

644



picoplatin  
ZD0437  
AMD-437



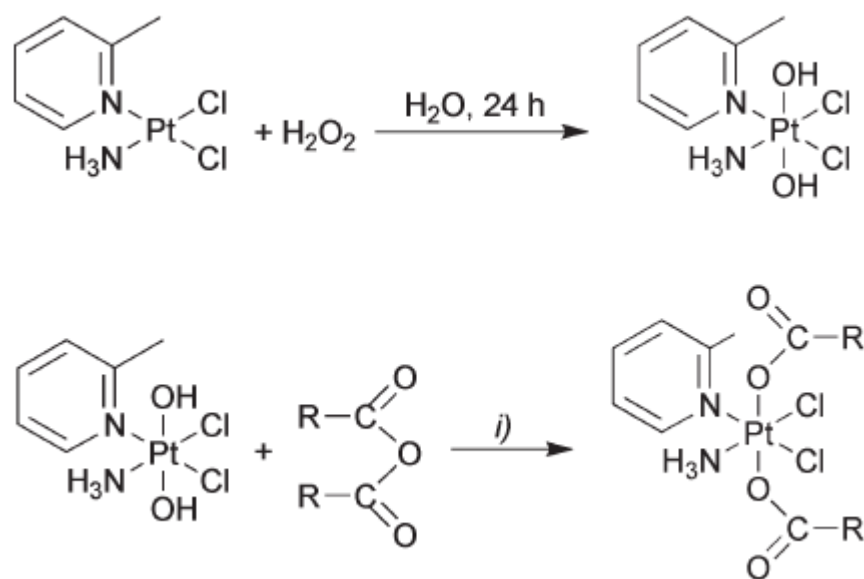
- 1 L = CH<sub>3</sub>COO<sup>-</sup>
- 2 L = CH<sub>3</sub>CH<sub>2</sub>COO<sup>-</sup>
- 3 L = CH<sub>3</sub>(CH<sub>2</sub>)<sub>2</sub>COO<sup>-</sup>
- 4 L = CH<sub>3</sub>(CH<sub>2</sub>)<sub>3</sub>COO<sup>-</sup>
- 5 L = CH<sub>3</sub>(CH<sub>2</sub>)<sub>4</sub>COO<sup>-</sup>

645

646

647

648 **Scheme 1.**



649

650

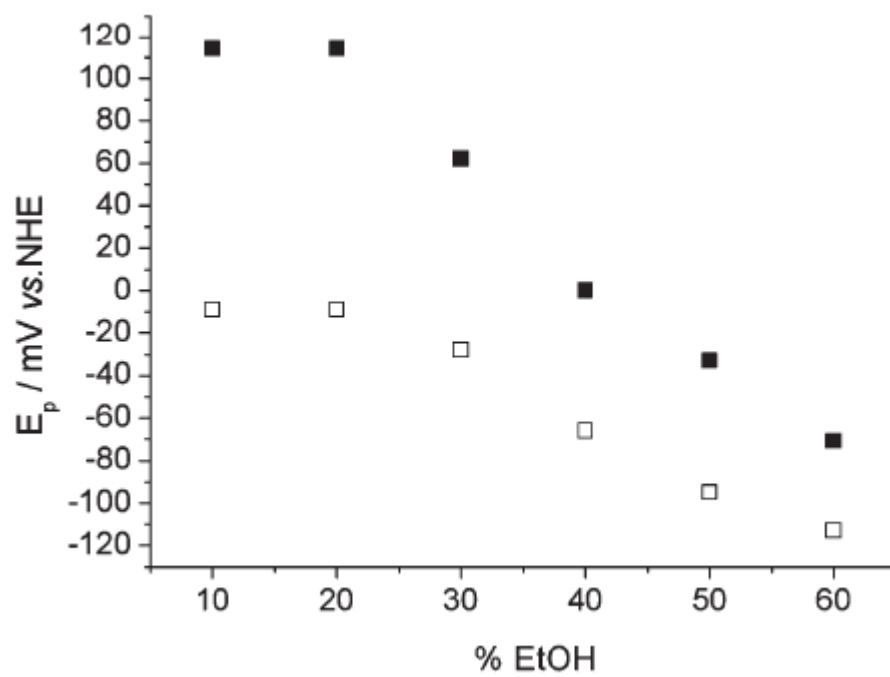
651





658 **Figure 4**

659

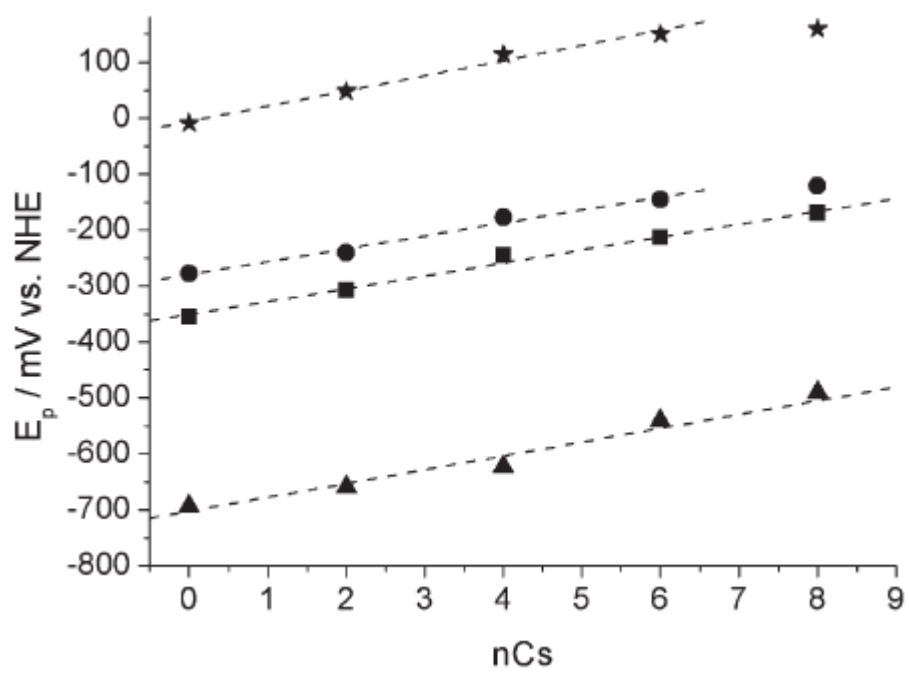


660

661

662 **Figure 5**

663

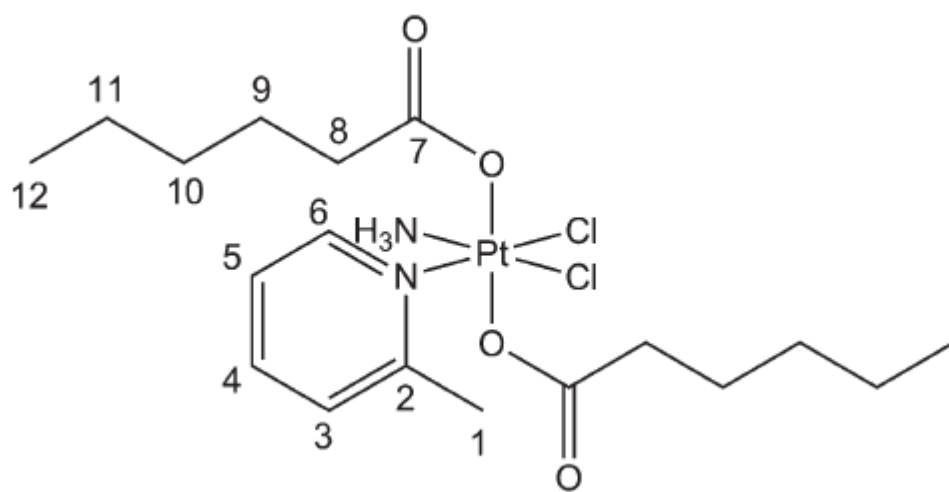


664

665

666 **Figure 6**

667



668

669